Journal of Theoretical and Applied Information Technology

31st December 2023. Vol.101. No 24

ISSN: 1992-8645 www.jatit.org E-ISSN: 1817-3195

METHODS OF MODELING, CALCULATION AND ANALYSIS OF ROBOTIC SYSTEMS FROM COMPOSITE MATERIALS UNDER DYNAMIC INFLUENCES

KAMIL KHAYRNASOV[1]

[1]Department of Digital Technologies and Information Systems,

Moscow Aviation Institute (National Research University), Moscow, Russian Federation

E-mail: [1]khayrnasov_mai@mail.ru

ABSTRACT

The methods of modeling, calculation and analysis of a robotic system are considered: a semi-natural simulation stand designed to imitate flight characteristics in ground conditions. The originality of this study is in the uniqueness of the design of the stands and the modeling of the stand from a composite material. A method has been developed for approximating bearings, gearboxes and gear rims by rod systems identical to them in terms of rigidity. A method for creating a stand of maximum rigidity by locating the base of composite material along the lines of maximum stresses has been developed. A study of composite of materials and magnesium alloy, traditionally used in the manufacture of stands for dynamic operational loads, was made. A method for creating a three-layer stand structure that provides maximum strength and rigidity has been developed. The problem by the finite element method is solved. The convergence of the results of the study was determined by thickening the mesh of finite elements and comparing the results obtained. The stress-strain state of stands made of composite material and magnesium alloy has been obtained. Comparison of the results shows that the stand made of composite material has advantages over the stand made of magnesium alloy. A layer-by-layer stress state of a five-layer composite material has been obtained. The results of the failure of the composite were determined based on the proven criteria for the failure of layered materials. The considered research methods are applicable to a wide class of robotic systems under dynamic influences, containing bearings, gear rims, gearboxes and motors. The study revealed the structure of the arrangement of the base layers of the composite material, in which the construction has the greatest strength and rigidity. The production of dynamic stands from a composite material exceeds the strength characteristics of the magnesium alloy traditionally used in the manufacture of stands.

Keywords: *Robotic Systems; Stands; Composite Materials; Calculation; Analysis; Finite Element Method; Dynamic Effects*

1. INTRODUCTION

Robotic systems used in various fields of science and technology are complex systems that require a large amount of theoretical and experimental research for development and manufacture [1-5]. Therefore, the development of methodologies for modeling and analyzing such systems is an important and urgent problem. Robotic systems, in addition to standard parts, contain systems that are difficult to model in numerical simulation systems, for example, in the finite element method. Their real approximation leads to models with an unreasonably large number of equations that do not meet the identification requirements. Such systems include bearings, gear rims and gearboxes [6-10]. In existing calculation programs, there are models for identifying such systems. At the same time, they do not fully satisfy the real parameters of these systems. This study proposes a method for identifying bearing supports, gearboxes and gear rims by rod systems corresponding to them in terms of rigidity. One of the main factors for the efficient operation of robotic systems is the low inertial characteristics of the elements of robotic systems, which can be achieved using materials of high specific strength. Such materials include homogeneous ones: magnesium or composite material that changes its stiffness characteristics depending on the location of the base layers in a multilayer composite material.

We consider a three-stage simulation stand (Figure 1), consisting of a base connected to the forward fork by means of a gear rim, a pitch channel located in the forward fork on bearings and a roll channel located in the pitch channel by means of a gear connection. The stand is designed to imitate the flight of the test product in ground conditions. Multistage dynamic stands have all the attributes of robotic systems: degrees of freedom, bearings, gear rims, gearboxes and control centers. If the approximation of the bench elements by finite elements is not particularly difficult, then the approximation of such elements as bearing supports, gearboxes and gear rims is a difficult task that requires the creation of a program for calculating the stiffness of these elements and identifying them in the model [11-13]. In this study, the method developed by the author is used, consisting in the replacement of bearings, gearboxes and gear rims with a system of rod elements identical in rigidity to the replaced elements of the stand structure. The cited and available literature sources discuss studies of individual structural elements: three-layer plates, bearings, characteristics of a multilayer composite material, etc. There are practically no studies of the product as a whole with the interaction and influence of the component parts of the product. This work studies the effect of fiber orientation of a carbon fiber composite material on the mechanical properties. The structure of fiber orientation of a carbon fiber composite material has been identified, in which the layers have the lowest stresses and, therefore, the greatest strength and rigidity, which affect the positioning accuracy of dynamic structures, one of the main characteristics of the efficiency of robotic systems. The destruction criteria are considered. According to these criteria, the destruction of an individual layer leads to the destruction of the multilayer material as a whole. The layers with the highest stresses, stress characteristics and their direction have been identified.

The strengths of the manuscript include the developed methods and programs for the comprehensive study of dynamic stands made of composite material. The weaknesses of the manuscript are the insufficient number of available experimental results.

Figure 1. Three-stage stand for semi-natural imitation of a frame structure

2. MATERIALS AND METHODS

We imitate a three-degree bench of simulation and approximate it with finite elements. To model the stand, we use the simulation module and use rods, strips and shells, including three-layer ones with external carrier layers and filler located between them, preventing the outer carrier layers from approaching and absorbing shear stresses of the three-layer structure. The stand contains shells of complex curvature, three-dimensional elements at the base of the stand [13-15]. When modeling the stand, it should be taken into account that a multilayer composite material is used [16-18], the characteristics of which depend on the location of the weft and the composite warp in the multilayer structure. In addition, it is necessary to arrange the basis of the composite material along the trajectories of maximum stresses in order to obtain the structure of maximum rigidity; therefore, these trajectories must be determined from the solution of a stand made of a homogeneous material, that is, to imitate a stand from a homogeneous material, apply operational loads. Having obtained the trajectories of the location of maximum stresses, we place the composite material along the lines of maximum

ISSN: 1992-8645 www.jatit.org E-ISSN: 1817-3195

stresses. Next, we determine the trajectories of maximum stresses for a stand made of composite material and correct the location of the base layers of the multilayer composite material. These iterations are carried out until the location of the base of the composite material coincides with the trajectories of the maximum stresses of the stand under the action of operational loads.

The convergence of the results of the bench approximation under the action of operational loads is carried out by thickening the mesh of finite elements and if the results of the displacements of the nodal points of the previous approximation do not differ from the finer division of the structure by no more than 3%, we can assume that the results converge and the approximation of the previous division is sufficient to obtain accurate results. The Figure 2 shows a model of a three-stage dynamic bench, shown in Figure 1, approximated by finite elements and a section of this model.

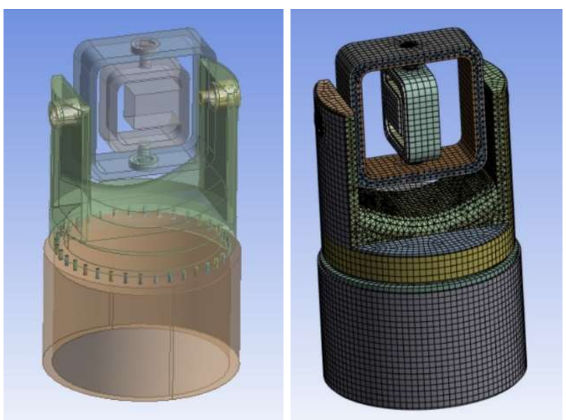

(a) (b)

Figure 2. (a) Model of a three-stage stand for semi-natural imitation of a frame structure; (b) Finite element approximation of model

A composite material is used as a material for the manufacture of the stand. To use it, it is necessary to determine its characteristics, which depend on the arrangement of warp and weft layers in a multilayer composite structure.

2.1 Equation

To solve the problem, we use the Lagrange equations. These equations make it possible to obtain the stress-strain state of robotic systems under dynamic influences. To do this, it is necessary to determine the kinetic and potential energy of the system under consideration and the work of external forces:

$$\frac{\partial}{\partial t}\frac{\partial T}{\partial \dot{q}_k} + \frac{\partial U}{\partial q_k} = Q, \qquad (1)$$

where T is the kinetic energy of deformation, U is the potential energy of deformation, q is the vector of generalized displacements, the index k is the number of degrees of freedom, t is time, the dot above the letter means differentiation with respect to time.

2.2 Relation Between Stresses-Strains

In the present study, the stand material is a composite material. There are two approaches to identify the relation between stresses and strains for a multilayer composite material, when the base of the layers is located at different angles: the method of reduced stiffnesses and taking into account the dependence for each layer separately. The reduced stiffness method used in this study calculates the generalized characteristics of a multilayer composite material characteristic of a homogeneous material. In the method under consideration, the relation between stresses and strains for each layer of a multilayer composite material and the number of resolving equations depends on the number of layers of the multilayer composite, which leads to an increase in the resolving equations as for the method of reduced characteristics multiplied by the number of layers of the multilayer composite. This approach leads to an unreasonably large number of resolving equations, an increase in computational errors and is practically not used when considering large structures, which also includes a multi-degree bench for semi-natural simulation.

We consider a method for obtaining the above characteristics of a multilayer composite material with different angles of the base of the layers. In a plane stressed state of an anisotropic material, the relation between stresses and strains, if the coordinate axes coincide with the anisotropy axes, can be written as:

$$\{\sigma\} = [E]\{\varepsilon\}, \qquad (2)$$

where

$$\{\sigma\}^T = \{\sigma_s, \sigma_\theta, \sigma_{s\theta}\},$$
$$[E] = \begin{Bmatrix} Q_{11} & Q_{12} & 0 \\ Q_{21} & Q_{22} & 0 \\ 0 & 0 & Q_{66} \end{Bmatrix}, \qquad (3)$$
$$\{\varepsilon\}^T = \{\varepsilon_s, \varepsilon_\theta, \varepsilon_{s\theta}\},$$

$$Q_{11} = \frac{E_s}{1-v_{s\theta}v_{\theta s}},\ Q_{12} = \frac{v_{s\theta}E_s}{1-v_{s\theta}v_{\theta s}},$$
$$Q_{21} = \frac{v_{\theta s}E_s}{1-v_{s\theta}v_{\theta s}},\ Q_{22} = \frac{E_\theta}{1-v_{s\theta}v_{\theta s}},\ Q_{66} = G_{66}.$$

when the composite material layer is rotated through an angle θ, the stress-strain matrix will have the following form:

$$[\bar{E}] = \begin{Bmatrix} \bar{Q}_{11} & \bar{Q}_{12} & \bar{Q}_{16} \\ \bar{Q}_{21} & \bar{Q}_{22} & \bar{Q}_{26} \\ \bar{Q}_{61} & \bar{Q}_{62} & \bar{Q}_{66} \end{Bmatrix}, \quad (4)$$

where the following is denoted:

$$\begin{aligned} &\bar{Q}_{11} = c^4Q_{11} - s^4Q_{22} + 2(Q_{12} + 2Q_{66})s^2c^2, \\ &\bar{Q}_{12} = (Q_{11} + Q_{22} - 4Q_{66})s^2c^2 + (s^2+c^2)Q_{22}, \\ &\bar{Q}_{16} = (c^2Q_{11} - s^2Q_{12} + (Q_{12} + 2Q_{66})(s^2-c^2))sc, \\ &\bar{Q}_{22} = s^4Q_{11} - c^4Q_{22} + 2(Q_{12} + 2Q_{66})s^2c^2, \\ &\bar{Q}_{26} = (s^2Q_{11} - c^2Q_{12} - (Q_{12} + 2Q_{66})(s^2-c^2))sc, \\ &\bar{Q}_{66} = (Q_{11} - 2Q_{12} + Q_{22})s^2c^2 + (s^2-c^2)Q_{66}, \end{aligned} \quad (5)$$

The deformation of a layer located at a distance z from the middle surface can be written as:

$$\{\varepsilon\} = \{\varepsilon^o\} + z\{\chi^o\}, \quad (6)$$

where $\{\varepsilon^o\}$ are membrane deformations of the median surface, $\{\chi^o\}$ are deformations of curvature of the median surface.

Substituting the resulting expression into equation **Error! Reference source not found.**, we write:

$$\{\sigma\} = [\bar{Q}]\{\varepsilon^o\} + z[\bar{Q}]\{\chi^o\}. \quad (7)$$

We express the normal forces *N* and the bending moments *M* in terms of stresses and strains:

$$\begin{aligned} &\{N\} = \int_{-h/2}^{h/2}\{\sigma\}dz, \{N\}^T = (N_s, N_\theta, N_{s\theta}), \\ &\{M\} = \int_{-h/2}^{h/2}\{\sigma\}zdz, \{M\}^T = (M_s, M_\theta, M_{s\theta}). \end{aligned} \quad (8)$$

As a result, by integrating equation **Error! Reference source not found.**, we obtain the following dependencies:

$$\begin{aligned} &\begin{Bmatrix} N \\ M \end{Bmatrix} = [E]\begin{Bmatrix} \varepsilon^o \\ \chi^o \end{Bmatrix}, \\ &[E] = \begin{bmatrix} [A] & [B] \\ [B] & [D] \end{bmatrix}, \\ &[A] = \begin{bmatrix} A_{11} & A_{12} & A_{16} \\ A_{21} & A_{22} & A_{26} \\ A_{61} & A_{62} & A_{66} \end{bmatrix}, \\ &[B] = \begin{bmatrix} B_{11} & B_{12} & B_{16} \\ B_{21} & B_{22} & B_{26} \\ B_{61} & B_{62} & B_{66} \end{bmatrix}, \\ &[D] = \begin{bmatrix} D_{11} & D_{12} & D_{16} \\ D_{21} & D_{22} & D_{26} \\ D_{61} & D_{62} & D_{66} \end{bmatrix}, \\ &\{A_{ij}, B_{ij}, D_{ij}\} = \int_{-h/2}^{h/2} Q_{ij}(1, z, z^2)\, dz, \\ &i,j = 1,2,3. \end{aligned} \quad (9)$$

In the case of constant parameters of layers of composite materials, from expression **Error! Reference source not found.** we obtain:

$$\begin{aligned} &A_{ij} = \sum_{k=1}^{n} \bar{Q}_{ij}(h_k - h_{k-1}), i,j = 1,2,6, \\ &B_{ij} = \sum_{k=1}^{n} \bar{Q}_{ij}(h^2{}_k - h^2{}_{k-1}), i,j = 1,2,6, \\ &D_{ij} = \sum_{k=1}^{n} \bar{Q}_{ij}(h^3{}_k - h^3{}_{k-1}), i,j = 1,2,6, \end{aligned} \quad (10)$$

where A_{ij}, B_{ij}, D_{ij} are membrane, flexural-membrane and flexural stiffnesses.

Figure 3 shows the notation used in equations **Error! Reference source not found.**.

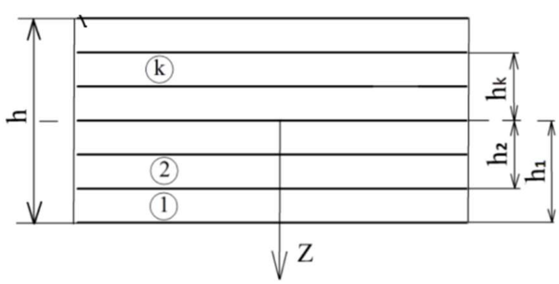

Figure 3. Structure and notation for multilayer composite material

2.3 Three-Layer Shell

We consider a three-layer shell used in the construction of robotic systems to increase rigidity and reduce weight characteristics [19]. The use of three-layer shells in robotic systems makes it possible to reduce the inertial characteristics of structural elements and thereby increase the positioning accuracy and efficiency of dynamic systems. Modeling of three-layer shells consists of external load-bearing layers and a filler layer between the load-bearing layers, mainly preventing shear stresses and the approach of the load-bearing layers. The parameters of the given characteristics of the carrier layers consisting of a multilayer composite material are calculated according to the method given above. To take into account shear deformations in the filler, the stiffness matrix is supplemented with shear stiffness parameters.

$$\begin{Bmatrix}\sigma_4\\ \sigma_5\end{Bmatrix}^{(k)} = \begin{Bmatrix}\bar{Q}_{44} & 0\\ 0 & \bar{Q}_{55}\end{Bmatrix}\begin{Bmatrix}\bar{\varepsilon}_4\\ \bar{\varepsilon}_5\end{Bmatrix}^{(k)}, \quad (11)$$

where $\bar{Q}_{44} = G_{13}, \bar{Q}_{55} = G_{23}$, are shear modules.

When solving the problem of a three-layer shell structure, the displacements of the carrier layers are calculated on the basis of which the displacements and angles of rotation of the filler normal are determined. In this case, the dependence of the filler displacements can be linear, quadratic or cubic. In the present study, this dependence is determined by the broken line law. Denoting the total thickness of the three-layer package through t, the thicknesses of the outer bearing layers throught_1 and t_2, and the thickness of the filler t_3, we write the displacement dependences and the angles of rotation of the normal of the neutral axis of the filler in the following form:

$$v_3 = \frac{\bar{v}_1+\bar{v}_2}{2}, \varphi_3 = \frac{\bar{v}_1-\bar{v}_2}{t}, \bar{v}_1 = v_1 - \frac{t_1 e_{13}}{2},$$
$$\bar{v}_2 = v_2 + \frac{t_2 e_{23}}{2}. \quad (12)$$

For the filler layer located at a distance z from the neutral axis of the three-layer package, these dependences have the following form:

$$v_2(z) = v_1 + z\varphi_3 = \frac{1}{2}\left(v_1 - \frac{t_1 e_{13}}{2} + v_2 + \frac{t_2 e_{23}}{2}\right) + \frac{z}{t_3}\left(v_1 - \frac{t_1 e_{13}}{2} - v_3 - \frac{t_2 e_{23}}{2}\right),$$
$$u_3(z) = u_1 + z\varphi_3 = \frac{1}{2}\left(u_1 - \frac{t_1 e_{13}}{2} + u_2 + \frac{t_2 e_{23}}{2}\right) + \frac{z}{t_3}\left(u_1 - \frac{t_1 e_{13}}{2} - u_2 - \frac{t_2 e_{23}}{2}\right), \quad (13)$$
$$w_3(z) = w_3 + \frac{z}{t_3}(w_2 - w_1).$$

The designations adopted for the three-layer shell are shown in the **Error! Reference source not found.**.

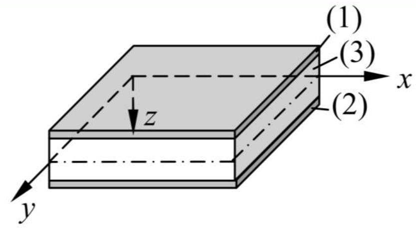

Figure 4. Three-layer shell

2.4 Method for Determining the Structure of a Composite Material

The multilayer composite material changes its characteristics depending on the location of the warp and weft of the composite yarns. To obtain the maximum rigidity of a multilayer composite material, it is necessary to position the base of the composite material in the direction of the maximum stresses acting in the structure under study under the action of operational loads. In this case, part of the layers in the multilayer composite material should be made at an angle to the maximum stresses to absorb shear stresses. The ratio of the arrangement of layers in a multilayer composite material is a complex task that requires a large number of theoretical and experimental studies. And it depends on the structure under study and the operating loads.

This study proposes an iterative method for arranging layers of a multilayer composite material along lines of maximum stresses. At the first stage, a model of a structure made of a homogeneous material under the action of operational loads is investigated. As a result of the study, we obtain the trajectories of maximum stresses. At the second stage, the structure model is made of a composite material with the arrangement of layers of a multilayer composite material along the lines of maximum stresses. The trajectories of maximum stresses obtained as a result of the studies make it possible to correct the location of the composite base and carry out the calculation of the structure. In this way, the location of the base of the composite material along the lines of maximum stresses is achieved and, thereby, a model of the structure of maximum strength and rigidity is obtained. Layers with an angle to the trajectories of maximum stresses for the perception of shear stresses are determined from the results of the analysis of the stress-strain state of the structure.

The multilayer composite material changes its characteristics depending on the location of the

ISSN: 1992-8645 www.jatit.org E-ISSN: 1817-3195

warp and weft of the composite yarns. To obtain the maximum rigidity of a multilayer composite material, it is necessary to position the base of the composite material in the direction of the maximum stresses acting in the structure under study under the action of operational loads. In this case, part of the layers in the multilayer composite material should be made at an angle to the maximum stresses to absorb shear stresses. The ratio of the arrangement of layers in a multilayer composite material is a complex task that requires a large number of theoretical and experimental studies. And it depends on the structure under study and the operating loads.

This study proposes an iterative method for arranging layers of a multilayer composite material along lines of maximum stresses. At the first stage, a model of a structure made of a homogeneous material under the action of operational loads is investigated. As a result of the study, we obtain the trajectories of maximum stresses. At the second stage, the structure model is made of a composite material with the arrangement of layers of a multilayer composite material along the lines of maximum stresses. The trajectories of maximum stresses obtained as a result of the studies make it possible to correct the location of the composite base and carry out the calculation of the structure. In this way, the location of the base of the composite material along the lines of maximum stresses is achieved and, thereby, a model of the structure of maximum strength and rigidity is obtained. Layers with an angle to the trajectories of maximum stresses for the perception of shear stresses are determined from the results of the analysis of the stress-strain state of the structure.

2.5 Modeling Technique for Gear Rims, Gearboxes and Bearings

In this study, a method for approximating such elements of robotic systems as bearings, gear rims and bearing supports is proposed. The approximation technique is as follows. The rigidity of the specified elements is determined on the basis of the developed program using the formulas of the mechanics of machines and mechanisms. Next, a bar structure of the corresponding stiffness is modeled and the ring gear, bearing or ring gear is replaced in the model with a bar structure of the same stiffness. The performed calculations and studies have shown the validity of this technique. The results of comparison with the available experimental studies of showed the good agreement.

2.6 Modeling and Approximation of the Stand

The stand is a three-layer shell structure, consisting of a stand model made of lightweight composite material (Table 1) with outer load-bearing layers of a five-layer composite material with a layer orientation of 0/45/0/-45/0 degrees. The stand was approximated by finite elements. Gear rims, bearing supports and gearboxes were approximated by bar structures of appropriate stiffness. The convergence of the results was determined by condensing the number of finite elements: the structure model was divided into *n* finite elements, the calculation was carried out, and the obtained results were compared with the results obtained by splitting into *1.5n* finite elements. If the results differed by no more than 3%, splitting into *n* finite elements was considered sufficient to obtain acceptable results.

Table 1. Physical and mechanical characteristics of carbon fiber

Modulus of elasticity, MPa	Poisson's ratio	Shear modulus, MPa	Tensile strength, MPa	Ultimate compressive strength, MPa	Bending strength, MPa	Density, kg/m^3
0.85×10^5	0.27	0.82×10^4	395	240	470	1518

3. RESULTS

To solve the problem: a robotic system made of composite materials under the action of dynamic loads [19-25], it is necessary to determine the trajectories of maximum stresses. To do this, we consider an identical design consisting of a homogeneous material: magnesium. Having determined and positioned the basis of the layers of the multilayer composite material along the lines of maximum stresses according to the method described in Section 2, we will study the bench from the composite material based on the equations:

$$[M]\{\ddot{q}\} + [K]\{q\} = \{Q\} - [N_{nl}], \quad (14)$$

where $[M]$ is the mass matrix; $\{\ddot{q}\}$ are generalized accelerations, the dot above the letter means time differentiation; $[K]$ is the stiffness matrix; $\{q\}$ are generalizes displacements; $\{Q\}$ is the vector of external forces; $[N_{nl}]$ are nonlinear terms of the strain-displacement dependence calculated from the results of previous loading steps.

The solution of a geometrically nonlinear problem consists of the following steps. At the first loading step, the nonlinear term of equation **Error! Reference source not found.** is not taken into account. At the second loading step, the nonlinear term is calculated from the generalized displacements calculated at the first loading step. For the third and subsequent loading steps, nonlinear terms are calculated from the results of generalized displacements obtained at previous loading steps by quadratic or cubic interpolation to improve the convergence of the results. When solving problems of dynamic action, it is necessary to set an insignificant initial displacement. This displacement for the nodal points of the finite element approximation of the stand can be obtained, for example, from the solution of the problem of static loading of the stand, multiplied by 10^{-8}.When solving problems of dynamic loading of structures, for the convergence of results, it is necessary to compare the results obtained at adjacent loading steps, and if these results differ by more than 3%, it is necessary to halve the loading step.

The Table 2 shows the maximum stresses in the layers of a five-layer composite material depending on the orientation of the layers. One layer is located on the surface of the model. An analysis of the obtained stresses of the bench at dynamic angular velocity showed that the most favorable arrangement of the orientation of the layers on the stress state of the structure under study corresponds to the first line of the Table 2.

Table 2. Influence of the orientation of the layers in a five-layer composite material on the maximum values of the stresses of the layers

Layer orientation	1st layer, MPa	2st layer, MPa	3st layer, MPa	4st layer, MPa	5st layer, MPa
0º/45º/0º/-45º/0º	60.2	96.23	31.36	71.2	26.7
0º/45º/90º/-45º/0º	63.9	64.60	132.3	54.3	29.4
0º/75º/0º/-75º/0º	60.4	117.2	57.23	92.5	21.8
0º/15º/90º/-15º/0º	57.2	39.3	135.9	26.0	21.6
0º/0º/90º/90º/0º	55.5	38.8	103.8	85.44	23.08

As we can see from the Table 2, the five-layer composite material in the stand under dynamic loading is the most durable, consisting of the orientation of the layers 0º/45º/0º/-45º/0º and 0º/0º/90º/90º/0º and the weakest when the layers are oriented 0º/15º/90º/-15º/0º, 0º/45º/90º/-45º/0º. Zero orientation corresponds to the direction of the trajectory of maximum stresses.

3.1 Rejection criteria

When studying the stress-strain state of a structure, especially when determining its load-bearing capacity, safety margins are determined: the ratio of the permissible stress to the effective stress or the ratio of the effective stress to its permissible value. The last relation is used in strength criteria in relation to multilayer materials with different load-bearing capacities of the layers. There are several proven strength criteria, named after their authors: Tsai-Wu, Tsai-Hill, Hoffman, Hashin, Park and criteria used at NASA: LaRC and Koons. The criteria have their advantages and disadvantages and are applied to various types of multilayer material compositions. Based on them, a multilayer composite material is calculated. We consider in more detail the criteria used in this study: Tsai-Wu, Tsai-Hill and Hoffman criteria for maximum stresses and strains [16-19]. The maximum stress and strain criterion is based on the excess of one of the ratios of effective stress to permissible stress or effective deformation to permissible deformation of the material:

$$\max\left\{\left|\frac{\sigma_x}{[\sigma_x]}\right|, \left|\frac{\sigma_y}{[\sigma_y]}\right|, \left|\frac{\sigma_z}{[\sigma_z]}\right|, \left|\frac{\tau_{xy}}{[\tau_{xy}]}\right|, \left|\frac{\tau_{xz}}{[\tau_{xz}]}\right|, \left|\frac{\tau_{yz}}{[\tau_{yz}]}\right|\right\} \le 1,$$
$$\max\left\{\left|\frac{\varepsilon_x}{[\varepsilon_x]}\right|, \left|\frac{\varepsilon_y}{[\varepsilon_y]}\right|, \left|\frac{\varepsilon_z}{[\varepsilon_z]}\right|, \left|\frac{\gamma_{xy}}{[\tau_{xy}]}\right|, \left|\frac{\gamma_{xz}}{[\tau_{xz}]}\right|, \left|\frac{\gamma_{yz}}{[\tau_{yz}]}\right|\right\} \le 1. \quad (15)$$

Here $\sigma_x, \sigma_y, \sigma_z$ are normal stresses; $\varepsilon_x, \varepsilon_y, \varepsilon_z$ are normal deformations; $\tau_{xy}, \tau_{xz}, \tau_{yz}$ are tangential stresses in the corresponding plane; $\gamma_{xy}, \gamma_{xz}, \gamma_{yz}$ are shear deformations in the corresponding planes, expressions in square brackets mean the permissible values of the corresponding deformations and stresses. Tsai-Wu, Tsai-Hill, and Hoffman tests are quadratic tests and are calculated based on a second-order polynomial depending on the type of coefficients Aij and Ai.

ISSN: 1992-8645 www.jatit.org E-ISSN: 1817-3195

$$F = A_{11}\sigma_x^2 + A_{22}\sigma_y^2 + A_{33}\sigma_z^2 + A_{44}\tau_{xy}^2 + A_{55}\tau_{xz}^2 + A_{66}\tau_{yz}^2 + 2A_{xy}\sigma_x\sigma_y + 2A_{xz}\sigma_x\sigma_z + 2A_{yz}\sigma_y\sigma_z + A_1\sigma_x + A_2\sigma_y + A_3\sigma_z \leq 1. \quad (16)$$

When the value of this polynomial is less than or equal to one, it is assumed that failure of the multilayer material does not occur. For a plane stress state in this polynomial, it is necessary to assume that σz = 0.

3.2 Tsai-Wu criterion

The coefficients in this criterion are calculated from the relations:

$$A_{11} = \frac{1}{[\sigma_{xt}][\sigma_{xc}]}\ ; \quad A_{22} = \frac{1}{[\sigma_{yt}][\sigma_{yc}]}\ ; \quad A_{66} = \frac{1}{[\tau_{yz}^2]}\ ;\ A_1 = \frac{1}{[\sigma_{xt}]} - \frac{1}{[\sigma_{xc}]}\ ;\ A_2 = \frac{1}{[\sigma_{yt}]} - \frac{1}{[\sigma_{yc}]}, \quad (17)$$

where the index t means tension, and c is compression.

Here $\sigma_x = \sigma_y = P$, and other expressions are equal to zero.

$$A_{xy} = \frac{1}{2P^2}\left[1 - P\left(\frac{1}{[\sigma_{xt}]} - \frac{1}{[\sigma_{xc}]} + \frac{1}{[\sigma_{yt}]} - \frac{1}{[\sigma_{yc}]}\right) - P^2\left(\frac{1}{[\sigma_{xt}][\sigma_{xc}]} + \frac{1}{[\sigma_{yt}][\sigma_{yc}]}\right)\right]. \quad (18)$$

3.3 Hoffman criterion

For this criterion, the coefficient Aij is determined from the relation:

$$A_{12} = \frac{1}{[\sigma_{xt}][\sigma_{xc}]}, \quad (19)$$

and the Hoffman destruction criterion takes the form:

$$\frac{\sigma_x^2}{[\sigma_{xt}][\sigma_{xc}]} + \frac{\sigma_y^2}{[\sigma_{yt}][\sigma_{yc}]} - \frac{\sigma_x\,\sigma_y}{[\sigma_{xt}][\sigma_{xc}]} + \frac{\sigma_x}{[\sigma_{yt}][\sigma_{yc}]} + \frac{\sigma_y}{[\sigma_{yt}][\sigma_{yc}]} \leq 1. \quad (20)$$

3.4 Tsai-Hill criterion

Coefficients are calculated from the ratios:

$$A_{11} = \frac{1}{[\sigma_x]^2}\ ;\ A_{22} = \frac{1}{[\sigma_y]^2}\ ;\ A_1 = 0\ ;\ A_2 = 0\ ;\ A_{12} = \frac{1}{[\sigma_x]^2}, \quad (21)$$

and the failure criterion has the form:

$$\frac{\sigma_x^2}{[\sigma_x]^2} + \frac{\sigma_y^2}{[\sigma_y]^2} + \frac{\tau_{xy}^2}{[\tau_{xy}]^2} - \frac{\sigma_x\,\sigma_y}{2[\sigma_x]^2} \leq 1. \quad (22)$$

The criteria used in this study are the most general and widely used in studying the load-bearing capacity of multilayer composite structures. The disadvantages of Tsai-Hill criterion are that it does not take into account the different values of the tensile and compressive strength of the material. All failure criteria presented assume that if a layer fails according to the corresponding criterion, then the entire multilayer material fails. The considered destruction criteria are used in various calculation programs.

The **Error! Reference source not found.** shows stress mosaic and the strain an angular velocity of the heading channel of 600 deg/s.

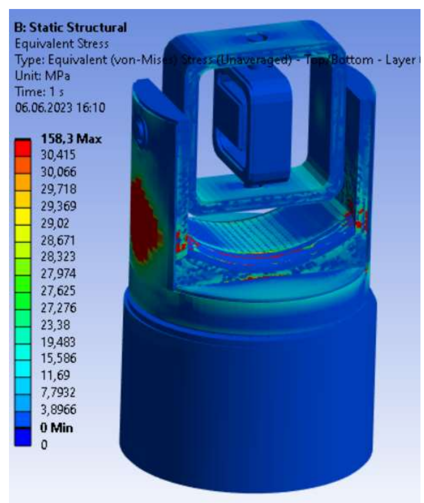

(a)

ISSN: 1992-8645 www.jatit.org E-ISSN: 1817-3195

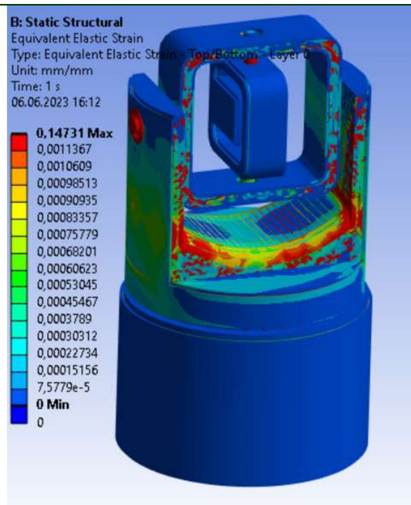

(b)

Figure 5. (a) stress mosaic; (b) strain mosaic at an angular velocity of the heading channel of 600 deg/s

The Figures 6-8 show the stresses in the layers of a five-layer three-axial composite material located in the directions 0/45/0/-45/0 degrees. The directions are counted from the axis located along the lines of maximum stresses obtained when calculating the bench from a homogeneous material.

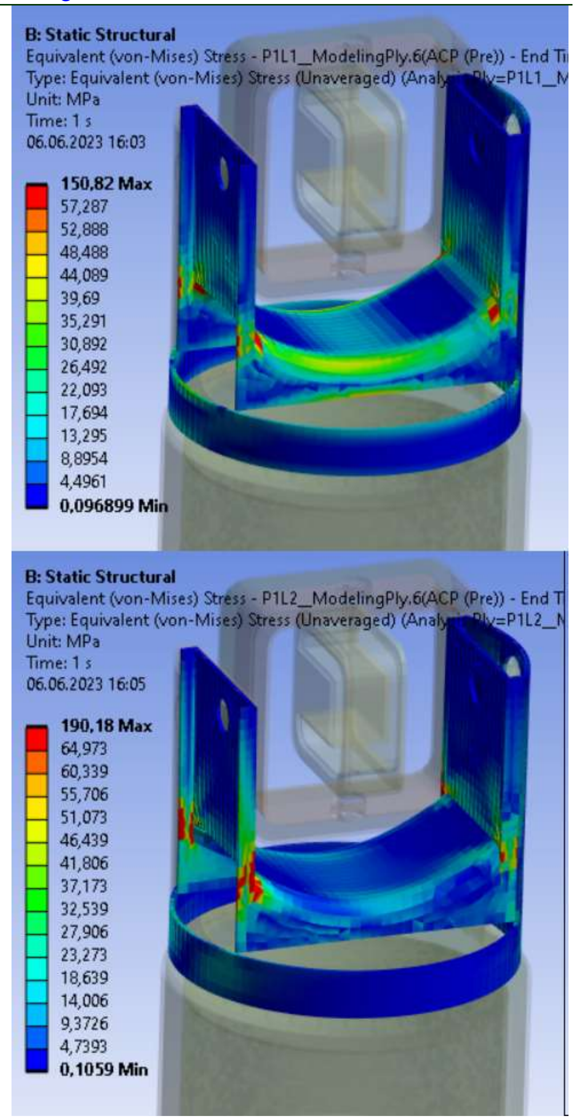

Figure 6. Stresses in 1 and 2 layers of composite material

ISSN: 1992-8645 www.jatit.org E-ISSN: 1817-3195

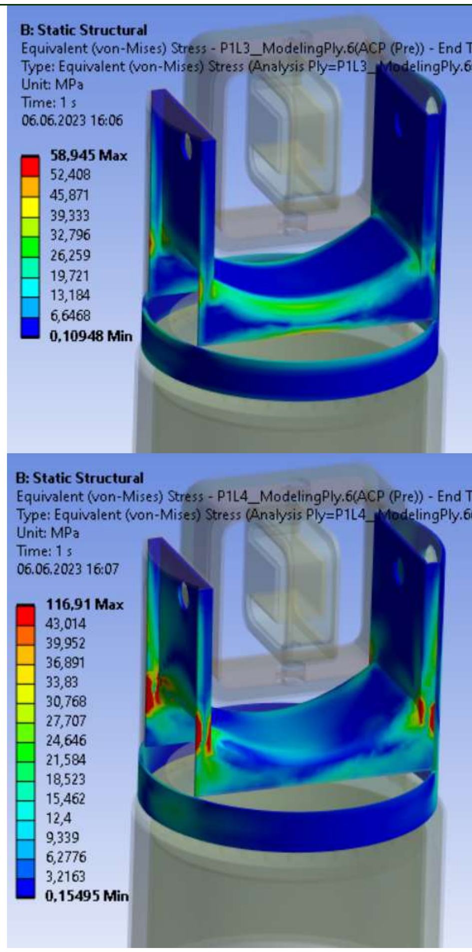

Figure 7. Stresses in 3 and 4 layers of composite material

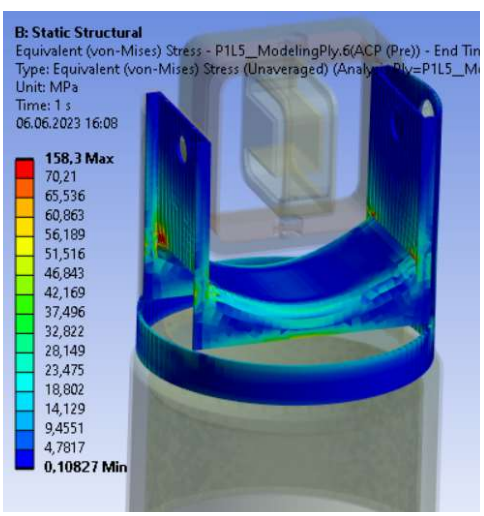

Figure 8. Stresses in layer of composite material

Figure 9 shows the stresses in the most loaded areas layer by layer. The following theories of destruction of multilayer composite materials were considered in the calculations: Tsai-Wu (tw), Tsai-Hill (th) and Hoffman (ho) [26-30]. In parentheses, the designation of theories of destruction in the Figure 9 is indicated. In the Figure 9, the following designations are accepted: e - stress, 2 - direction, t - tension, in parentheses there is the number of the layer of a five-layer three-axial composite material. The layer numbering starts from the shell surface along the normal, i.e., the higher the layer number, the further it is from the surface. The notation tw(4) means that failure can occur in the fourth layer according to Tsai-Wu failure theory.

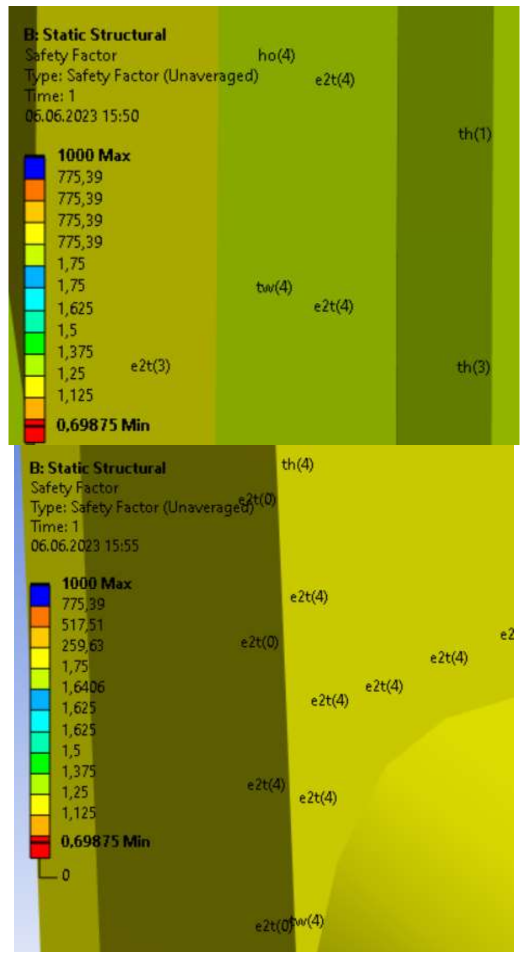

Figure 9. Maximum stresses and theories of destruction of layers of five-layer triaxial composite material, with the arrangement of layers at angles to the trajectories of maximum stresses 0/45/0/-45/0 degrees

As a result of the study, the stress-strain state of a three-degree stand for semi-natural modeling of a frame structure made of a composite material and a magnesium alloy was obtained under dynamic impact. The operational load of the angular velocity was used as a dynamic effect. The Figure 5 show a mosaic of the stress-strain state and the strain of the elements of a carbon fiber stand at an angular velocity of the course channel of 650 deg/s. Similar results were obtained for a stand made of magnesium material. Comparison of movements of stands made of magnesium and composite materials showed that the maximum stress of a stand made of magnesium is 10% more than for a stand made of composite. The mass of the stand made of composite is 12% less than the mass of the stand made of magnesium. Considering that the allowable stresses of unidirectional carbon fiber are 1.3-1.5 times higher than the allowable stresses of magnesium alloy, we can say that the use of composite materials for HIL simulation stands is a promising direction, so research in this area is important and relevant. The difference from the previous work is that the work carried out research on the orientation of the base layers of a five-layer composite material for load-bearing capacity. The structure of the arrangement of the base layers of carbon fiber composite material has been identified, in which the structure has the lowest stresses and, therefore, the greatest strength and rigidity, which affect the positioning accuracy of dynamic structures, one of the main characteristics of the efficiency of robotic systems. The criteria for destruction of multilayer materials are considered. According to the destruction criteria, the destruction of an individual layer leads to the destruction of the multilayer material as a whole, therefore it is important to identify the structure of the multilayer composite material in which the stresses of the layers have the minimum characteristics among the structures considered. The orientation of the layers is measured from the trajectories of the maximum stresses obtained when solving the problem of a magnesium alloy.

4. CONCLUSIONS

The conducted studies have shown that the manufacture of robotic systems from composite materials with high specific strength characteristics, in comparison with homogeneous materials, allows reducing the inertial characteristics of the elements of the moving parts of robotic systems, which helps to increase their dynamism, and this is one of the main operational characteristics of such structures. The paper presents a method for determining the reduced characteristics of a multilayer composite material. A technique has been developed for obtaining the maximum rigidity and strength of a structure from a composite material. The method is based on the location of the base layers of a multilayer composite material in a structure along the trajectories of maximum stresses. The developed method for approximating the elements of robotic systems, such as gear rims, bearings and gearboxes by a system of rod systems, made it possible to calculate the stress-strain state of a semi-natural simulation bench made of magnesium and a composite material under the action of an inertial operational dynamic load. The analysis of the obtained results showed that the maximum stress of the stand made of magnesium is 12% higher than the maximum stresses of the stand made of composite material. The presented methods are applicable to a wide class of robotic systems that include bearings, gear rims and gearboxes. As a result of the work carried out, methods for modeling, calculation and analysis of robotic systems made of composite material under operational loads were developed, and a study was carried out on the stress-strain state of robotic systems: multi-degree dynamic benches of semi-natural modeling under operational loads. Methods have been developed for determining the load-bearing capacity of the stand, taking into account all the elements that operate the stand. Currently, multi-degree dynamic stands are made of magnesium alloys, and composite materials with higher specific strength characteristics are not used. Therefore, research in this area is important and relevant. Directions for future research include the development of methods for the kinematic behavior of robotic systems, calculation and analysis of natural frequencies of oscillations.

ACKNOWLEDGEMENT

This work was supported financially by the Russian Science Foundation under the Scientific Project № 22-29-20299 (the recipient is K.Z. Khayrnasov, https://rscf.ru/project/22-29-20299/).

REFRENCES

[1]. Tian, Y.; Chen, C.; Sagoe-Crentsil, K.; Zhang, J.; Duan, W. Intelligent robotic systems for structural health monitoring: Applications and future trends. *Autom. in Constr.* 2022, *139*, 104273. https://doi.org/10.1016/j.autcon.2022.104273

[2]. Tao, B.; Feng, Y.; Fan, X.; Zhuang, M.; Chen, X.; Wang, F.; Wu, Y. Accuracy of dental implant surgery using dynamic navigation and robotic systems: An in vitro study. *J. of Dent.* 2022, *123*, 104170. https://doi.org/10.1016/j.jdent.2022.104170 robotic

ISSN: 1992-8645 www.jatit.org E-ISSN: 1817-3195

[3]. Xu, X.; Chen, Y.; Zou, B.; Gong, Y. Assignment of parcels to loading stations in robotic sorting systems. Transportation *Res. Part E: Log. and Transp. Rev.* 2022, *164*, 102808. https://doi.org/10.1016/j.tre.2022.102808

[4]. Boschetti, G.; Faccio, M.; Granata, I.; Minto, R. 3D collision avoidance strategy and performance evaluation for human–robot collaborative systems. *Comp. & Industr. Eng.* 2023, *179*, 109225. https://doi.org/10.1016/j.cie.2023.109225

[5]. Lindqvist, B.; Karlsson, S.; Koval, A.; Tevetzidis, I.; Haluška, J.; Kanellakis, C.; Nikolakopoulos, G. Multimodality robotic systems: Integrated combined legged-aerial mobility for subterranean search-and-rescue. *Robot. and Autonom. Syst.* 2022, *154*, 104134. https://doi.org/10.1016/j.robot.2022.104134

[6]. Guo, Y.; Parker, R.G. Stiffness matrix calculation of rolling element bearings using a finite element/contact mechanics model. *Mechan. and Mach. Theory* 2012, *51*, 32-45. https://doi.org/10.1016/j.mechmachtheory.2011.12.006

[7]. Hoopert, I. Advanced analytical approach for calculating ball and roller bearings. *J. of Tribol.* 2014, *136*, 11105-11116.

[8]. Childs, P.R. Rolling Element Bearings In *Mechanical Design*; Elsevier Ltd.: Oxford, UK, 2021

[9]. Dewangan, P.; Parey, A.; Hammami, A.; Chaari, F.; Haddar, M. Dynamic characteristics of a wind turbine gearbox with amplitude modulation and gravity effect: Theoretical and experimental investigation. *Mechan. and Mach. Theory* 2022, *167*, 104468.

[10]. Liu, L.; Zhu, L.; Gou, X. Modeling and analysis of load distribution ratio and meshing stiffness for orthogonal spur-face gear drive under point contact. *Mechan. and Mach. Theory* 2023, *182*, 105239. https://doi.org/10.1016/j.mechmachtheory.2023.105312

[11]. Zienkiewicz, O.C.; Taylor, R.L.; Zhu, J.Z. *Finite element method: its basis and fundamental*; Butterworth-Heinemann: Oxford, UK, 2013.

[12]. Barbero, E.J. *Finite Element Analysis of Composite Materials using Abaqus®*; CRC press: Boca-Raton, USA, 2023.

[13]. Moaveni, S. *Finite Element Analysis Theory and Application with ANSYS*; Pearson Education: London, UK, 2015.

[14]. Koutromanos, I. *Fundamentals of finite element analysis: linear finite element analysis*; John Wiley & Sons: New York, UK, 2018)

[15]. Bathe, K.J. *Finite element procedures*; Pearson education Inc.: New York, UK, 2006.

[16]. Vasiliev, V.V.; Morozov, E.V. *Advanced mechanics of composite materials and structures*; Elsevier: Cambridge, UK, 2018.

[17]. Gavva, L.M.; Firsanov, V.V. Investigation Method of the Static Strength of Structurally-Anisotropic Composite Panels According to a Refined Theory. *Mech. of Compos. Mat.* 2023, *59(2)* 1-16.

[18]. Mitrofanov, O.V. Current problems and basic relationships for investigations of composite panels with asymmetric structure taking into account geometric nonlinearity. *Nat. and Eng. Sci.* 2021, *2*, 140-144.

[19]. Latyshev, O.G.; Veremeychik, A.B.; Zhukov, E.A. *Application of composite materials in stands for dynamic loading*; Publishing house of MSTU N.E. Bauman: Moscow, Russia, 2011.

[20]. Manes, A.; Gilioli, A.; Sbarufatti, C.; Giglio, M. Experimental and numerical investigations of low velocity impact on sandwich panels. *Compos. Struct.* 2013, *99*, 8-18. https://doi.org/10.1016/j.compstruct.2012.11.031.

[21]. Kim, H.-G.; Wiebe, R. Numerical investigation of stress states in buckled laminated composite plates under dynamic loading. *Compos. Struct.* 2018, *235*, 111743. https://doi.org/10.1016/j.compstruct.2019.111743

[22]. Phadnis, V.A.; Silberschmidt, V.V. *8.14 Composites under dynamic loads at high velocities*; Elsevier: Cambridge, UK, 2018.

[23]. Correas, A.C.; Ghasemnejad, H. Analytical development on impact behaviour of composite sandwich laminates by differentiated loading regimes. *Aerosp. Sci. and Techn.* 2022, 126, 107658. https://doi.org/10.1016/j.ast.2022.107658 1270-9638/

[24]. Noman, A.A.; Shohel, S.M.; Riyad, S.H.; Gupta, S.S. Investigate the mechanical strength of laminated composite carbon fiber with different fiber orientations by numerically using finite element analysis. *Mater. Tod.: Proceed.* 2023, preprint. https://doi.org/10.1016/j.matpr.2023.02.132

[25]. Lin, J.P.; Liu, X.; Wang, Y.; Xu, R.; Wang, G. Static and dynamic analysis of three-

layered partial-interaction composite structures. *Eng. Struct.* 2022, *252*, 113581. https://doi.org/10.1016/j.engstruct.2021.113581

[26]. Zhang, B.; Ge, J.; Cheng, F.; Huang, J.; Liu, S.; Liang, J. Failure prediction for fiber reinforced polymer composites based on virtual experimental tests. *J. of Mat. Res. and Techn.* 2023, *24*, 8924-8939.

[27]. Daniel, I.; Werner, B.; Fenner, J.; Cho, J.M. Mechanical and failure behavior of composite materials under static and dynamic loading. In 50th AIAA/ASME/ASCE/AHS/ASC Structures, Structural Dynamics and Materials Conference, USA, 14 June 2009. https://doi.org/10.2514/6.2009-2425

[28]. Gu, J.; Chen, P.; Su, L.; Li, K. A theoretical and experimental assessment of 3D macroscopic failure criteria for predicting pure inter-fiber fracture of transversely isotropic UD composites. *Comp. Struct.* 2021, *259*, 113466.

[29]. Sun, Q.; Zhou, G.; Meng, Z.; Guo, H.; Chen, Z.; Liu, H.; Kang, H.; Keten, S.; Su, X. Failure criteria of unidirectional carbon fiber reinforced polymer composites informed by a computational micromechanics model. *Comp. Sci. and Techn.* 2019, *172*, 81-95. https://doi.org/10.1016/j.compscitech.2019.01.012.

[30]. Gunyaev, G.M.; Zhigun, I.G.; Dushin, M.I.; Vorontsov, I.A.; Yakushin, V.A.; Rumyantsev, A.F. Dependence of elastic and strength characteristics of high-modulus composites on reinforcement schemes. *Polym. Mech.* 1974, *6*, 1019-1027.